Microchimica Acta (2019) 186: 69
https://doi.org/10.1007/s00604-018-3178-7

ORIGINAL PAPER

A nanocomposite consisting of porous graphitic carbon nitride nanosheets and oxidized multiwalled carbon nanotubes for simultaneous stripping voltammetric determination of cadmium(II), mercury(II), lead(II) and zinc(II)

Manikandan Ramalingam [1] · Vinoth Kumar Ponnusamy [1,2] · Sriman Narayanan Sangilimuthu [3]

Received: 18 September 2018 / Accepted: 12 December 2018 / Published online: 9 January 2019

Abstract

A 3D nanocomposite consisting of porous graphitic carbon nitride nanosheets (p-g-C_3N_4-NSs) and oxidized multiwalled carbon nanotubes (O-MWCNTs) was prepared by simultaneous chemical oxidation of bulk g-C_3N_4 and bulk MWCNTs. This one-step oxidation results in the formation of acidic functional groups on the basal surfaces of both g-C_3N_4 and MWCNTs. Simultaneously, the O-MWCNTs are incorporated in-situ on the porous structure of p-g-C_3N_4. The acid functionalization and surface morphology of the nanocomposite were examined using attenuated total reflectance infrared spectroscopy, X-ray diffraction, and high-resolution transmission electron microscopy. The nanocomposite was used to modify a screen-printed electrode (SPE) which then was studied by using cyclic voltammetry, electrochemical impedance spectroscopy, and differential pulse voltammetry. The modified SPE exhibits excellent sensitivity and selectivity towards the simultaneous detection of the heavy metal ions Cd(II), Hg(II), Pb(II) and Zn(II), typically at −0.78, +0.35, −0.5 and − 1.16 V (vs. Ag/AgCl). The detection limits (at S/N = 3) range between 8 and 60 *n*g L^{-1} under conditions of stripping analysis. The method was applied to the simultaneous detection of these ions in various (spiked) food samples. The results demonstrated the good accuracy and reproducibility of the method.

Keywords Porous g-C_3N_4 · Oxidized-MWCNTs · 3D Nanocomposite · Screen-printed electrode · Stripping analysis · Simultaneous detection · Heavy metals · Food analysis

Introduction

Heavy metals including cadmium (Cd), lead (Pb), mercury (Hg) and zinc (Zn) profoundly affect the environmental system including water and soil [1]. They also can enter the food chain and pose significant threats to living creatures [2]. WHO regulated the presence of heavy metal levels in drinking water such as 0.003 mg L^{-1} for Cd, 2.0 mg L^{-1} for Cu, 0.01 mg L^{-1} for Pb and 0.001 mg L^{-1} for Hg [3]. Hence, even at trace levels of heavy metals present in drinking water or food can cause significant health issues to humans [4]. Therefore, it is crucial to develop an efficient, sensitive and selective determination of heavy metals in foods samples.

Various analytical methods have been reported for the detection of heavy metal ions in food. They include spectrophotometry [5], surface enhanced raman spectroscopy [6], inductively coupled plasma mass spectroscopy [7], atomic absorption spectroscopy [8], chromatography [9] and electrochemical methods [10–12]. Among different techniques, electrochemical methods, particularly differential pulse stripping voltammetry (DPSV) is considered as a more suitable tool for the determination of heavy metals due to its sensitivity,

Electronic supplementary material The online version of this article (https://doi.org/10.1007/s00604-018-3178-7) contains supplementary material, which is available to authorized users.

✉ Vinoth Kumar Ponnusamy
kumar@kmu.edu.tw

[1] Department of Medicinal and Applied Chemistry, Kaohsiung Medical University, Kaohsiung City-807, Taiwan

[2] Research Center for Environmental Medicine, Kaohsiung Medical University, Kaohsiung City-807, Taiwan

[3] Department of Analytical Chemistry, School of Chemical Sciences, University of Madras, Guindy Campus, Chennai City, Tamil Nadu 600 025, India

selectivity, rapidity, and low-cost. Chemically modified electrodes are received high importance among researches for heavy metal analysis. Moreover, anodic stripping voltammetric detection methods have been widely used for heavy metal analysis using mercury constructed electrodes such as dropping mercury electrode (DME), hanging mercury drop electrode (HMDE) [10] and mercury film electrodes [11]. These electrodes are considered as toxic and high-cost, and further, there are risks associated with the use and disposal of mercury [12]. Therefore, to overcome these difficulties, it is essential to develop mercury-free electrodes for electrochemical determination of heavy metals.

Graphitic carbon nitrides (g-C_3N_4) have received prodigious application in the field of electrochemical sensors due to its unique planar structure and distinctive mechanical and electrocatalytic properties [13–18]. g-C_3N_4 (2D) possess sp^2 bonded carbon and nitrogen similar to graphene along with π-electrons in the layered structure [13]. g-C_3N_4 based electrochemical sensors has been reported for various electroanalytical determinations. To enhance the electrical conductivity of g-C_3N_4, it has been composited with various metal nanoparticles, polymers, and carbon based materials [16–18]. *Hongying lv* et al. reported ion flux measurement platform for heavy metals using carbon nitride heterojunction film modified carbon fiber microelectrode [14]. *Gao* et al. reported g-C_3N nanosheets/Nafion electrode for Cd determination in various samples [15]. Voltammetric determination of ultra-trace Pb in water samples using EDTA immobilized graphene-like g-C_3N has been reported by *Teng* et al. [16]. Nevertheless, g-C_3N_4 shows poor electrical conductivity and thereby limits its application towards electrochemical sensors. In the past two decades, multiwalled carbon nanotubes (MWCNTs, 1D dimension) based electrochemical sensors were exhibited several impressive electrochemical properties due to its prominent specific surface area, fast electron transfer rate, good adsorption property and minimal electrode surface fouling [19, 20]. Based on the above-aforementioned properties, we attempted to explore the fabrication of porous g-C_3N_4 with MWCNTs to achieve a novel 3D nanocomposite material with synergetic properties of g-C_3N_4 (high electrocatalytic activity) and MWCNTs (high electronic conductivity) for electrochemical sensor application. MWCNTs (1D) structure in the nanocomposite (3D) increases the electrical conductivity of the g-C_3N_4 (2D) by enhancing electron-transfer rate between g-C_3N_4 and MWCNTs.

In this work, the porous g-C_3N_4/oxidized(O)-MWCNTs nanocomposite was prepared by one-step chemical oxidation method. The preparation of this 3D nanocomposite was facile due to the strong π-π stocking and electrostatic interactions between g-C_3N_4-NSs (2D) and O-MWCNTs (1D). The prepared P-g-C_3N_4/O-MWCNTs composite was characterized by various techniques such as attenuated total reflectance infrared spectroscopy (ATR-IR), X-ray diffraction (XRD), and high-resolution transmission electron microscopy (HR-TEM). Further, the P-g-C_3N_4/O-MWCNTs composite was drop cast on the screen-printed electrode (SPE) and electrochemically characterized by different techniques like cyclic voltammetry, electrochemical impedance spectroscopy, and differential pulse voltammetry techniques. To the best of our knowledge, till now P-g-C_3N_4/O-MWCNTs composite has not been explored for heavy metals determination by electroanalytical methods. The prepared P-g-C_3N_4/O-MWCNTs composite modified SPE exhibits excellent sensitive detection towards heavy metals in food samples.

Material and methods

Chemicals and materials

Melamine was purchased from Alfa-Aesar (USA) and multiwall carbon nanotubes were purchased from Sigma-Aldrich (USA, https://www.sigmaaldrich.com/). Sodium acetate, acetic acid, disodium hydrogen phosphate, dihydrogen sodium phosphate, potassium chloride were purchased from Xilong scientific Co. Ltd., (China, https://xilongchemical.en.made-in-china.com/). $K_4[Fe(CN)_6]$, $K_3[Fe(CN)_6]$, potassium dichromate, lead nitride, cadmium acetate, mercury chloride, copper chloride, and zinc chloride were purchased from Showa chemicals Co. Ltd. (Japan, https://www.showa-chemical.co.jp). Sulfuric acid and nitric acid were purchased from Fisher scientific company (UK, https://www.fishersci.co.uk). All the heavy metals solutions were prepared using ultra-pure water (18 MΩ·cm). Zensor screen-printed electrode (5 mm) single disk electrodes were purchased from Zensor R&D Corporation (Taiwan, http://www.zensor.com.tw/).

All the voltammetric experiments were carried out with CHI 210D electrochemical workstation (CHI Instruments Inc., USA, https://www.chinstruments.com/) coupled with Asus desktop computer. The three electrode system was used throughout electrochemical experiments. Ag/AgCl electrode served as a reference electrode, a platinum wire as an auxiliary electrode and Zensor screen-printed electrode (5 mm) was used as a working electrode. All the electrochemical measurements were carried in room temperature (24 ± 1 °C). pH was measured with Suntex pH meter (SP-2100, Taiwan) at room temperature (24 ± 1 °C), and ThermoScientific (USA, https://www.thermofisher.com) Heraeus Megafuge 8R centrifuge was used for centrifugation. Attenuated total reflectance infrared (ATR-IR) spectra were measured at Bruker Alpha model instrument (Germany). High-resolution transmission electron microscopy (HR-TEM) and selected area electron diffraction (SAED) images were observed at JEOL 3010 (Japan), and X-ray diffraction (XRD) were recorded at Bruker D8 advance (Germany).

Synthesis of porous g-C_3N_4/O-MWCNTs composite

The porous g-C_3N_4/O-MWCNTs composite was prepared by a one-step chemical oxidation method using potassium dichromate and sulfuric acid (Scheme 1). 10 g of potassium dichromate was added into 50 mL sulfuric acid (98%) in a 100 mL beaker under stirring condition. 0.5 g of bulk g-C_3N_4 (bulk g-C_3N_4 was prepared as similar to a previously reported method [21]) and 0.5 g MWCNTs were added in the oxidation mixture and then it was stirred for 24 h at room temperature. Then the oxidized mixture was slowly dispensed in 1 L of ultra-pure water and allowed to cool at room temperature. The mixture solution was washed with water and centrifuged at 6000 rpm (4025 rcf) several times (until pH becomes neutral) and then again washed with methanol and dried in a hot air oven at 50 °C for 3 h and used further.

Preparation of the screen-printed electrode (SPE) modified with porous g-C_3N_4/O-MWCNTs

5 mg of P-g-C_3N_4/O-MWCNTs composite was transferred to 5 mL of methanol followed by sonication for 30 min to disperse as a homogeneous solution. The solution was kept at room temperature for further use. 3 μL of the above mentioned P-g-C_3N_4/O-MWCNT composite was drop cast on the SPE surface followed by drying at room temperature and then used for further electrochemical analysis.

Preparation of food samples

All the vegetables (cabbage and capsicum) and food products (Noodles) were purchased from local markets. The vegetables were thoroughly washed with ultra-pure water several times and then dried in an oven at a temperature of 60 °C until dry. 1 g of vegetables were accurately weighed in a silica crucible and then heated on a hotplate to completely carbonize. Then, the sample was transferred to muffle furnace at 500 °C until the sample becomes dry ash. Next, the sample was allowed to attain room temperature, and then the ash sample was dissolved in 1:4 ratio of perchloric acid and nitric acid. Later, the sample solution was carefully transferred to a 20 mL volumetric flask with 0.5% of nitric acid solution [22]. Similarly, 1 g of noodle samples were accurately weighed and transferred to a silica crucible and then heated in a muffle furnace at 400 °C until the sample turned to dry ash. Then, the ash sample was dissolved in perchloric acid and nitric acid mixture (1:4 ratio) and transferred to a 25 mL volumetric flask. These sample solutions were used for the determination of heavy metals by differential pulse voltammetry (DPV). Same sample treatment procedure was followed for the preparation of 3 blanks.

Results and discussion

Choice of material

The 3D porous g-C_3N_4/O-MWCNTs nanocomposite were synthesized by single step chemical oxidation method. The synthesis of this nanocomposite was facile because of the strong π-π stocking and electrostatic interactions between g-C_3N_4-NSs (2D) and O-MWCNTs (1D). The negatively charged hydroxyl and carboxylic acids groups on the porous g-C_3N_4/O-MWCNTs/SPE plays a key role to the formation of complex with heavy metal ions (positive ions) due to the opposite charge interactions on the 3D porous structures (Scheme S1).

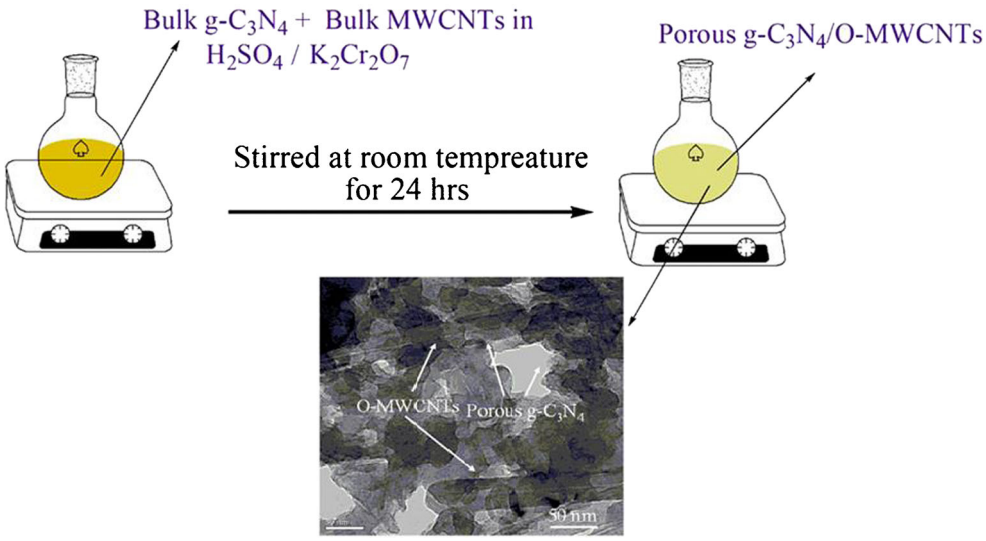

Scheme 1 Graphical representation of one-step preparation of porous g-C_3N_4/O-MWCNTs nanocomposite

Therefore, increase in the absorption capacity of porous g-C_3N_4/O-MWCNTs nanocomposite towards metal ions on the electrode surface which directly enhance the stripping peak current in terms of sensitivity and selectivity when compared with other reported composites for heavy metal analysis [13–18].

Surface morphology characterization

The surface morphology of the porous g-C_3N_4/O-MWCNTs composite was analyzed by HR-TEM techniques. Figure 1 TEM images of bulk g-C_3N_4 (Fig. 1a) shows agglomerated flakes and sheets morphology and P-g-C_3N_4/O-MWCNTs composites (Fig. 1b) indicates well-defined multiple atomic layers of g-C_3N_4 nanosheets incorporated with O-MWCNTs (multi-tubular and hollow structures), and Fig. 1c and d shows the lattice structure of porous g-C_3N_4/O-MWCNTs and SEAD patterns, The SEAD pattern was compared with XRD patterns and are matched. Hence, HR-TEM studies clearly indicate that this one-step synthetic method is facile and in-situ self-assembly of (strongly incorporate) O-MWCNTs on the basals of porous g-C_3N_4 nanosheets by π-π stacking and electrostatic interactions.

ATR-IR and XRD characterizations

The prepared porous g-C_3N_4/O-MWCNTs composites were further confirmed by ATR-IR technique. Figure S1 bulk g-C_3N_4 showed ATR-IR spectrum in the range of 3000–3500 cm^{-1} belongs to N-H stretching vibrations, 1800–900 cm^{-1} corresponding to Triazine ring of C-NH-C stretching and 807 cm^{-1} corresponds to breathing vibration mode of the s-triazine ring [23]. Figure 2a shows the expanded view spectrum of the g-C_3N_4 and porous g-C_3N_4/MWCNTs indicates the porous g-C_3N_4 absorption peaks were shifted (1236 to 1249 cm^{-1} and 1317 to 1327 cm^{-1}) around 13 cm^{-1} towards higher frequency range in the prepared composite. The 1406 cm^{-1} corresponds to C-OH functional group, and 1400 cm^{-1} corresponds to the stretching vibration of tertiary C-OH groups. The O-MWCNTs shows the IR rage of 1677 cm^{-1}, 1236 $cm^{-1,}$ and 1396 cm^{-1} corresponds to the C=C stretching vibration, C-O stretching vibration and carboxylic acid [20] bending vibrations respectively. Hence, the ATR-IR spectrum result clearly exhibits that hydroxyl and carboxylic acid group functionalized on the porous g-C_3N_4 composite.

The porous g-C_3N_4/MWCNTs were characterized by the X-ray diffraction method to analyze the lattice structure. Figure 2b shows the XRD pattern of MWCNTs, g-C_3N_4, and porous g-C_3N_4/MWCNTs composites. In bulk MWCNTs peak observed at 2θ ~26.1° is attributed to (002) reflection of carbon nanotubes. In the pattern of bulk g-C_3N_4, a strong peak located at 2θ~13.05 and 27.6° corresponds to (002) plane stemmed from the graphite-like layers stacked due to the weak Van der Walls force between porous g-C_3N_4 layers [23]. The diffraction patterns of O-MWCNTs and porous g-C_3N_4 matches well with JCPDS No. 26–1079 and 87–1526 respectively. In the porous g-C_3N_4/O-MWCNTs composite, the observed broadening of

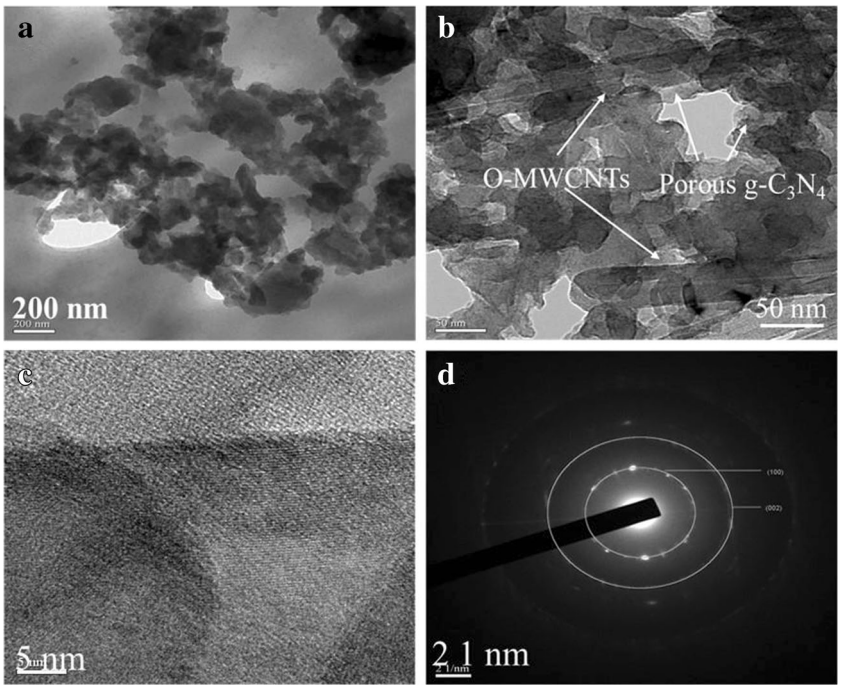

Fig. 1 HR-TEM images of **a** Bulk g-C_3N_4, **b** porous g-C_3N_4/O-MWCNTs, **c** Lattice structure of porous g-C_3N_4/O-MWCNTs composite and **d** SAED pattern of porous g-C_3N_4/O-MWCNTs

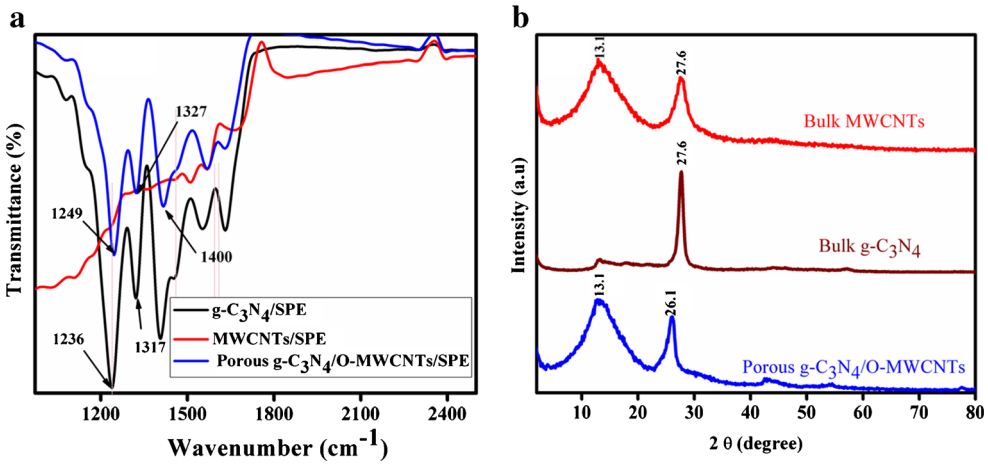

Fig. 2 **a** ATR-IR Spectrum for Bulk g-C_3N_4, MWCNTs, and porous g-C_3N_4/O-MWCNTs/SPE. **b** XRD patterns for bulk MWCNTs, bulk g-C_3N_4, and porous g-C_3N_4/O-MWCNTs

(002) plane at 2θ~27.6° may be due to the overlapping of diffraction from each moiety.

Electrochemical behavior of the modified SPE

The electrochemical behavior of different modified electrodes was studied using 5 mM of $[Fe(CN)_6]^{3-/4-}$ containing 0.1 M of KCl solution. Figure 3a shows the cyclic voltamograms (CV) of different electrodes in the potential range from −0.2 to 0.8 V was sweep at a scan rate of 50 mVs^{-1}. The different modified electrodes and its corresponding electrochemical parameters are shown in Table 1. In Fig. 3a, CV of bare SPE (black curve) shows the well-defined redox peak with lower ΔEp value, and the CV of SPE modified with bulk g-C_3N_4 (red curve) indicates the redox current peak has been decreased and the potential shifted slightly due to the semiconducting behavior of g-C_3N_4, the CV of SPE modified with bulk MWCNT's (sky blue curve) shows a higher redox peak currents with lower redox potential, and the CV of SPE modified with P-g-C_3N_4/O-MWCNT's/SPE (dark blue curve) shows higher ΔEp value due to modified electrode surface having negatively charged carboxylic acid and hydroxyl groups [24]. Figure 3b shows the EIS spectra of different modified electrodes, the semicircles correspond to electron transfer limited process, and its diameter are identical to electron transfer resistance. The R_{ct} value of P-g-C_3N_4/O-MWCNTs/SPE at Rct of 850 Ω, g-C_3N_4/SPE shows Rct at 628 Ω due to semiconductor property, MWCNTs/SPE showed Rct at 196 Ω because of strong electron transfer nature of MWCNTs and bare SPE showed Rct of 120 Ω. The cyclic voltammetry and EIS results clearly indicated that P-g-C_3N_4/O-MWCNTs/SPE surface possessed negatively charged hydroxyl and carboxylic acids groups.

Optimization

The following parameters were optimized: (a) Sample pH value; (b) preconcentration time. Respective data and Figures are given in the Electronic Supporting Material (Fig. S2 & S3). The following experimental conditions were found to give best results: (a) Best sample pH value: 5 in 0.1 M acetate buffer (b) Optimal preconcentration time: 240 s.

Analytical response of the modified SPE

After optimizing the different parameters including preconcentration time and pH conditions, the porous g-C_3N_4/O-MWCNTs/SPE was applied for the determination of

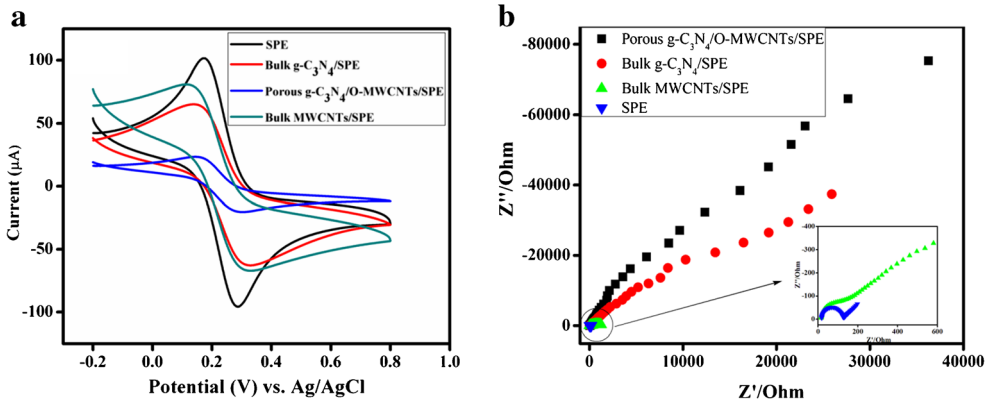

Fig. 3 **a** Electrochemical behavior of different modified electrodes in 5 mM $[Fe(CN)_6]^{3-/4-}$ in 0.1 M KCl as supporting electrolyte at a scan rate of 50 mV s^{-1}. **b** EIS of different modified electrodes in 5 mM $[Fe(CN)_6]^{3-/4-}$ in 0.1 M KCl as supporting electrolyte. Inset figure is zoom view of SPE

Table 1 The analytical parameters for determination of heavy metals using Porous g-C_3N_4/O-MWCNTs/SPE

Heavy metals	Linear range (μg L^{-1})	Linear equation	R^2	[a]LOD (μg L^{-1})
Hg	4.8 to 93.0	y = 10.02 × + 4.08	0.9875	0.04
Pb	0.35 to 6.5	y = 10.59 × +10.84	0.9939	0.008
	6.5 to 110	y = 85.60 × + 0.25	0.9983	
Cd	4.25 to 79.0	y = 03.57 × + 5.81	0.9960	0.03
	79.0 to 251	y = 27.17 × + 1.92	0.9989	
Zn	4.2 to 202.0	y = 08.16 × + 2.47	0.9928	0.06

[a] *LOD* limit of detection

heavy metals using differential pulse voltammetric techniques. Figure 4a shows the different modified electrode responses of bare/SPE, MWCNTs/SPE, bulk g-C_3N_4/SPE and P-g-C_3N_4/O-MWCNTs/SPE in 0.1 M acetate buffer (pH -5.0) containing 5 μg L^{-1} of Hg and 25 μg L^{-1} of Pb, Cd, Zn. The porous g-C_3N_4/O-MWCNTs/SPE showed higher stripping peak current compared to other electrodes due to the formation of metal ion-complexes on the electrode surface. Hence, P-g-C_3N_4/O-MWCNTs/SPE chosen for simultaneous determination of four heavy metals. Figure 4b shows P-g-C_3N_4/O-MWCNTs/SPE with different concentrations of metals (Hg, Pb, Cd, and Zn) in 0.1 M acetate buffer (pH -5.0) as supporting electrolyte and the results indicate that increases in the metal ions concentrations correspondingly increase in the anodic stripping currents. The corresponding calibration plots are shown in Fig. 4c–f, and linear ranges and detection

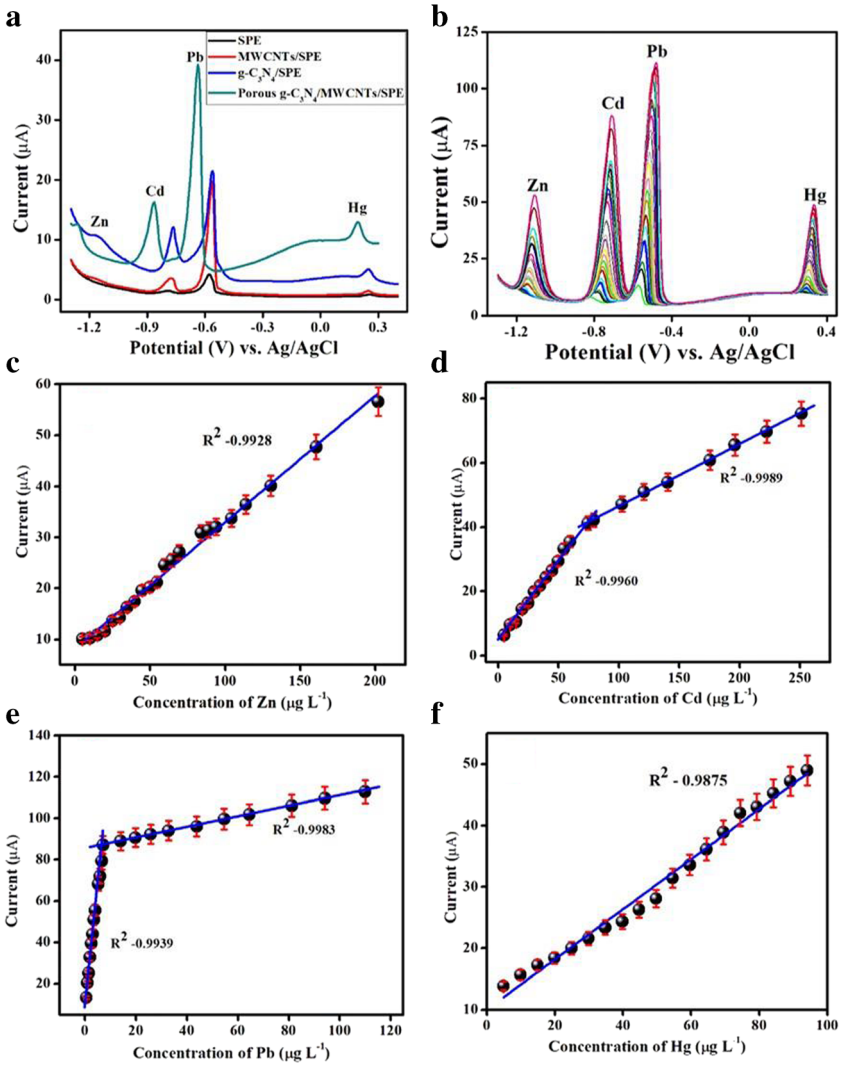

Fig. 4 **a** DPV response of different modified electrodes in 0.1 M acetate buffer (pH -5.0) containing 0.5 μg L^{-1} of Hg and 25 μg L^{-1} of Pb, Cd, Zn metals. Preconcentration time is 240 s and deposition potential are −1.3 V. **b** DPV response of porous g-C_3N_4/O-MWCNTs/SPE at different concentration of heavy metals in 0.1 M acetate buffer (pH -5.0) as supporting electrolyte, preconcentration time is 240 s and deposition potential is −1.3 V. **c–e** Calibration plots of different heavy metals (**c**-Zinc, **d**-Cadmium, **e**- lead, **f**- Mercury)

Table 2 Comparison of proposed modified electrode with previously reported methods

Modified electrode	Linear range (μg L^{-1})	LOD (μg L^{-1})	Electrolyte	Reference
Porous-g-C_3N_4/	Pb: 0.35 to 6.5			
O-MWCNTs/SPE	6.5 to 110	0.008	pH -5.0	This work
	Cd: 4.25 to 79.0			
	79.0 to 251	0.03		
	Zn: 4.2 to 202	0.06		
	Hg: 4.84 to 92	0.04		
Bi/AuNP's/SPE	Pb: 1 to 150	0.027		
	Cd: NM	NM	pH -4.5	[25]
	Zn: 1 to 150	0.055		
	Hg: NM	NM		
Bi/EG/GCE	Pb: 1 to 100	0.11		
	Cd: 1 to 100	0.18	pH -4.5	[26]
	Zn: 1 to 100	1.80		
	Hg: NM	NM		
RGO-Cs/PIL/GCE	Pb: 0.05 to 10	0.02		
	Cd: 0.05 to 10	0.01	pH -4.5	[27]
	Zn: NM	NM		
	Hg: NM	NM		
$Mo_6S_xI_9$-NWs/GCE	Pb: 1.50 to 450	0.45		
	Cd: 0.50 to 150	0.10	pH -4.7	[28]
	Zn: NM	NM		
	Hg: NM	NM		
Nf/PANI/SPE	Pb: 1 to 300	0.1		
	Cd: 1 to 300	0.1	pH -4.5	[29]
	Zn: 1 to 300	1.0		
	Hg: NM	NM		
rGO/Bi/CPE	Pb: 20 to 120	0.55		
	Cd: 20 to 120	2.8	pH -5.5	[30]
	Zn: 100 to 400	17.0		
	Hg: NM	NM		
Fe_2O_3/Gra/GCE	Pb: 1 to 100	0.07		
	Cd: 1 to 100	0.08	pH -5.0	[31]
	Zn: 1 to 100	0.11		
	Hg: NM	NM		
Activated Carbon	Pb: 0.5 to 2.25	0.1		
Fiber rod/GCE	Cd: 0.5 to 4.0	0.3	pH -4.2	[32]
	Zn: 1.0 to 4.0	1.0		
	Hg: NM	NM		
CeHCF/GCE	Pb: 2070 to 2,072,000	10		
	Cd: 1120 to 1,120,000	3	pH -5.0	[33]
	Zn: NM	NM		
	Hg: 2000 to 2,000,000	1000		

Porous g-C_3N_4/O-MWCNTs/SPE Porous Graphitic carbon nitride / Oxidized Multiwalled carbon nanotubes/ Screen printed electrode, Bi/AuNP's/SPE Bismuth/gold nanoparticle screen printed electrode, Bi/EG/GCE Electrochemically deposited graphene/bismuth nanocomposite film glassy carbon electrode, RGO-Cs/PIL/GCE reduced graphene oxide-chitosan/poly-L-lysine nanocomposite modified glassy carbon electrode, $Mo_6S_xI_9$-NWs Molybdenum-chalcogenide-halide nanowires modified glassy carbon electrode, Nf/PANI/SPE Nafion/graphene–polyaniline Nanocomposite screen-printed electrode, rGO/Bi/CPE reduced graphene oxide/Bi Nanocomposites/ carbon paste electrode, Fe_2O_3/Gra/GCE iron oxide/graphene Composite modified glassy carbon electrode, CeHCF/GCE Cerium Hexacyanoferrate modified glassy carbon electrode. NM-Not mentioned

limits are listed in Table 1. The achieved detection limits by the fabricated sensor showed better sensitivity than the earlier reported methods and the comparison results are showed in Table 2 [25–33].

Interference studies

The possible interferences during anodic stripping voltammetric determination of heavy metals have been analyzed. The selectivity is studied by fixing the concentration of heavy metals and adding an excess amount of interfering metal ions. Almost 10-fold excess of anions include F^-, SO_4^{2-} and 50-fold excess of NO_3^- did not show any influence on the stripping current of metal ions. Moreover, other possible interfering cations including NH_4^+, Mg^{2+}, Ca^{2+}, Ba^{2+}, and Al^{3+} were showed no interference at even excess concentrations, and they are generally inactive in voltammetry. Co^{2+} and Ni^{2+} are showed slight interference at 50-fold excess.

The anodic stripping voltammetric determination of heavy metals with copper has studied and the corresponding DPV responses are shows in Fig. 5a. The P-g-C_3N_4/O-MWCNTs/SPE with different concentrations of heavy metals and the corresponding stripping peak currents were increased. Moreover, the data was compared with the absences of copper ions, voltammograms of all the heavy metals showed well defined stripping peak currents. In the presences of copper ions, the voltammograms showed low stripping peak currents due to copper ions formed intermetallic alloy formation of Pb-Cu alloy [34]. During the analysis of heavy metals with copper, the anodic stripping peak potentials are negatively shifted, and the results are shown in Table S2. To avoid the intermetallic alloy formation in these steps, 0.1 mM of potassium ferrocyanide solution was added to form the copper ferrocyanide complexes, the solubility product of the copper ferrocyanide complex is Ksp-15.89 which is insoluble in the electrolyte [35].

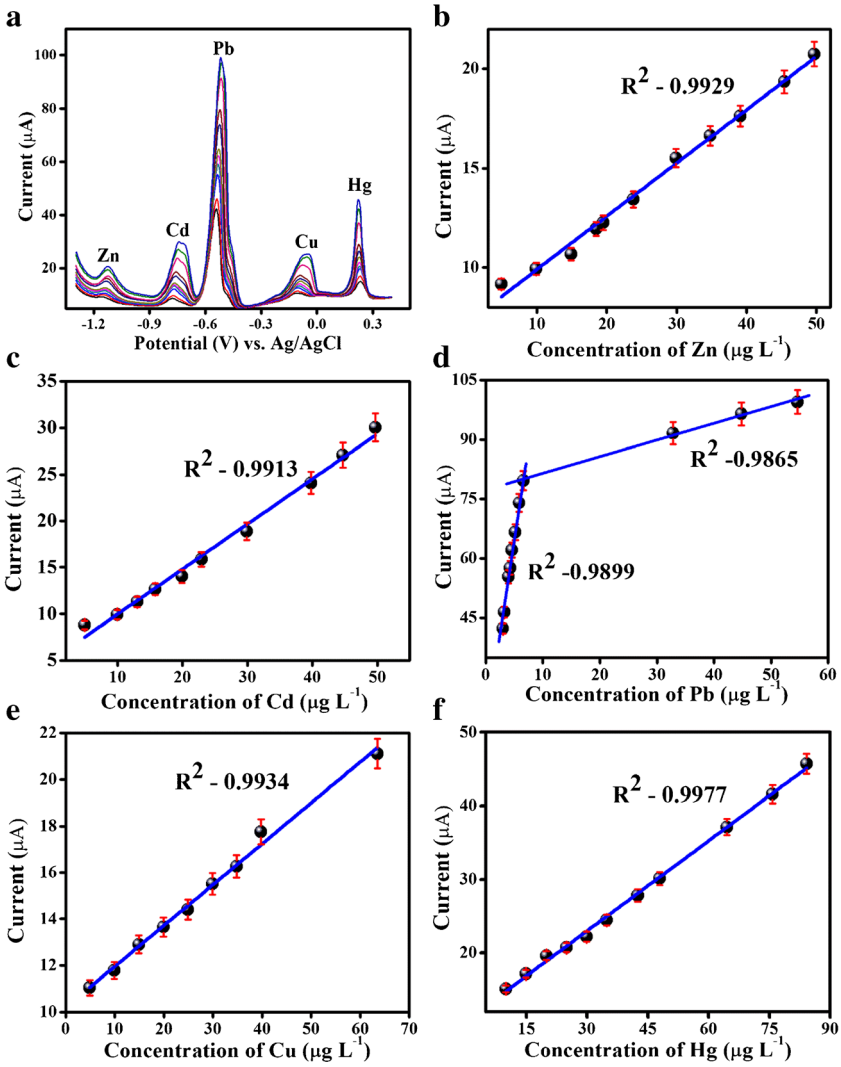

Fig. 5 **a** DPV response of porous g-C_3N_4/O-MWCNTs/SPE at different concentration of heavy metals with copper in 0.1 M acetate buffer (pH - 5.0) as supporting electrolyte, preconcentration time is 240 s and deposition potential is −1.3 V. **b** to **f** Calibration plots of different heavy metals (**b**-Zinc, **c**-Cadmium, **d**- lead, **e**- Copper and **f**- Mercury)

Stability and reproducibility

Stability and reproducibility of the porous g-C_3N_4/O-MWCNTs/SPE has been studied by six repetitive measurements of 25 μg L^{-1} of Pb and 50 μg L^{-1} of Hg, Cd, and Zn in 0.1 M acetate buffer pH -5.0. The anodic stripping peak currents of heavy metals are reproducible, with a relative standard deviation of 0.97%, 0.98%, 0.95% and 0.93% for zinc, cadmium, lead and mercury metals. The P-g-C_3N_4/O-MWCNTs/SPE showed excellent reproducibility towards anodic stripping voltammetric determination of heavy metals. The stability of the modified electrode has been studied over 9 days, and the anodic stripping peak current was measured, and the results are shown in figure S4. The P-g-C_3N_4/O-MWCNTs/SPE was kept in open air space while not in use.

Analysis of real samples

The fabricated P-g-C_3N_4/O-MWCNTs/SPE was successfully applied for the determination of heavy metals in different vegetables and noodles samples. The food samples were prepared by earlier discussed in section as in Material and Methods. All the samples were analyzed by spiking method. The results are summarized in Table S3.

Conclusion

A highly sensitive and selective electrochemical sensing platform for the simultaneous detection of four heavy metals based on 3D porous g-C_3N_4/O-MWCNTs nanocomposite modified SPE is reported. The 3D porous nanocomposite structure provided large surface area and active sites, while in-situ self-assembling of O-MWCNTs (1D) on the porous g-C_3N_4 (2D) nanosheets by strong π-π stocking and electrostatic interaction. The interconnection of O-MWCNTs (1D) offered continuous electron transfer pathways for efficient electroactive porous g-C_3N_4 (2D) nanosheets. The prepared porous g-C_3N_4/O-MWCNTs composite indicated excellent conductivity and electrocatalytic activity than bulk g-C_3N_4 and MWCNTs. The porous g-C_3N_4/O-MWCNTs/SPE has been successfully applied for towards simultaneous determination of four heavy metals by anodic stripping voltammetry method. The porous g-C_3N_4/O-MWCNTs/SPE showed excellent linear ranges and good selectivity and sensitivity. The fabricated electrode was applied for detection of heavy metals in real (food) samples and achieved satisfactory results. All these features exhibit that the 3D porous g-C_3N_4/O-MWCNTs nanocomposite is a promising nanomaterial in the field of metal ion sensor. Nonetheless, this study is limited with the detection of four heavy metal ions only in food sample matrices. Therefore, future work can be focused on the extended applications of this sensing platform to other metal ions and other sample matrices such as environmental, cosmetic and biological samples.

Acknowledgments The authors thank the Ministry of Science and Technology-Taiwan (MOST105-2113-M-037-019-MY2), Kaohsiung Medical University (KMU)-Taiwan and Research Center for Environmental Medicine-KMU, Taiwan for research grant supports.

Compliance with ethical standards The author(s) declare that they have no competing interests.

References

1. Cheng H, Hu Y (2010) Lead (Pb) isotopic fingerprinting and its applications in lead pollution studies in China: a review. Environ Pollut 158:1134–1146
2. Navas-Acien A, Guallar E, Silbergeld EK, Rothenberg S (2007) J Environ Health Perspect 115:472–476
3. World Health Organization Guidelines for Drinking-Water Quality, 4th edn, 2011. http://whqlibdoc.who.int/publications/2011/9789241548151_eng.pdf
4. Seiler HG, Sigel A, Sigel H (1998) Handbook on toxicity of inorganic compounds. Marcel-Dekker, New York
5. Tarighat MA (2016) Orthogonal projection approach and continuous wavelet transform-feed forward neural networks for simultaneous spectrophotometric determination of some heavy metals in diet samples. Food Chem 192:548–556
6. Cui L (2016) Surface-enhanced Raman spectroscopy for identification of heavy metal arsenic (V)-mediated enhancing effect on antibiotic resistance. Anal Chem 88:3164–3170
7. Dico G, Galvano ML, Dugo F, D'ascenzi G, Macaluso C, Vella A, Ferrantelli V (2018) Toxic metal levels in cocoa powder and chocolate by ICP-MS method after microwave-assisted digestion. Food Chem 245:1163–1168
8. Chen J, Chakravarty P, Davidson GR, Wren DG, Locke MA, Zhou Y, Brown G Jr, Cizdziel JV (2015) Simultaneous determination of mercury and organic carbon in sediment and soils using a direct mercury analyzer based on thermal decomposition–atomic absorption spectrophotometry. Anal Chim Acta 871:9–17
9. Solovyev N, Vinceti M, Grill P, Mandrioli J, Michalke B (2017) Redox speciation of iron, manganese, and copper in cerebrospinal fluid by strong cation exchange chromatography–sector field inductively coupled plasma mass spectrometry. Anal Chim Acta 973:25–33
10. Daňhel A, Havran L, Trnková L, Fojta M (2016) Hydrogen evolution facilitates reduction of DNA guanine residues at the hanging mercury drop electrode: evidence for a chemical mechanism. Electroanalysis 28:2785–2790
11. Brett CM, Fungaro DA (2000) Poly (ester sulphonic acid) coated mercury thin film electrodes: characterization and application in batch injection analysis stripping voltammetry of heavy metal ions. Talanta 50:1223–1231
12. Wang J (2005) Stripping analysis at bismuth electrodes: a review. Electroanalysis 17:1341–1346
13. Gan X, Zhao H, Schirhagl R, Quan X (2018) Microchim Acta 185: 478. https://doi.org/10.1007/s00604-018-3005-1
14. Lv H, Teng Z, Wang S, Feng K, Wang X, Wang C, Wang G (2018) Voltammetric simultaneous ion flux measurements platform for Cu^{2+}, Pb^{2+} and Hg^{2+} near rice root surface: utilizing carbon nitride

heterojunction film modified carbon fiber microelectrode. Sensors Actuators B 256:98–106
15. Gao W, Wang X, Li P, Wu Q, Qi F, Wu S, Ding K (2016) Highly sensitive and selective detection of cadmium with a graphite carbon nitride nanosheets/Nafion electrode. RSC Adv 6:113570–113575
16. Teng Z, Lv H, Wang L, Liu L, Wang C, Wang G (2016) Voltammetric sensor modified by EDTA-immobilized graphene-like carbon nitride nanosheets: preparation, characterization and selective determination of ultra-trace Pb (II) in water samples. Electrochim Acta 212:722–733
17. Balasubramanian P, Settu R, Chen SM, Chen TW (2018) Voltammetric sensing of sulfamethoxazole using a glassy carbon electrode modified with a graphitic carbon nitride and zinc oxide nanocomposite. Microchim Acta 185(8):396. https://doi.org/10.1007/s00604-018-2934-z
18. Zhang F, Zhong H, Lin Y, Chen M, Wang Q, Lin Y, Huang J (2018) A nanohybrid composed of Prussian blue and graphitic C3N4 nanosheets as the signal-generating tag in an enzyme-free electrochemical immunoassay for the neutrophil gelatinase-associated lipocalin. Microchim Acta 185(7):327. https://doi.org/10.1007/s00604-018-2865-8
19. Gooding JJ (2005) Nanostructuring electrodes with carbon nanotubes: a review on electrochemistry and applications for sensing. Electrochim Acta 50:3049–3060
20. Morton J, Havens N, Mugweru A, Wanekaya AK (2009) Detection of trace heavy metal ions using carbon nanotube-modified electrodes. Electroanalysis 21:1597–1603
21. Tian J, Liu Q, Ge C, Xing Z, Asiri AM, Al-Youbi AO, Sun X (2013) Ultrathin graphitic carbon nitride nanosheets: a low-cost, green, and highly efficient electrocatalyst toward the reduction of hydrogen peroxide and its glucose biosensing application. Nanoscale 5:8921–8924
22. Xu H, Zeng L, Huang D, Xian Y, Jin L (2008) A Nafion-coated bismuth film electrode for the determination of heavy metals in vegetable using differential pulse anodic stripping voltammetry: an alternative to mercury-based electrodes. Food Chem 109:834–839
23. Zhang H, Huang Y, Hu S, Huang Q, Wei C, Zhang W, Hao A (2015) Self-assembly of graphitic carbon nitride nanosheets–carbon nanotube composite for electrochemical simultaneous determination of catechol and hydroquinone. Electrochim Acta 176:28–35
24. Seenivasan R, Chang WJ, Gunasekaran S (2015) Highly sensitive detection and removal of lead ions in water using cysteine-functionalized graphene oxide/polypyrrole nanocomposite film electrode. Appl Mater Interfaces 7:15935–15943
25. Lu Z, Zhang J, Dai W, Lin X, Ye J, Ye J (2017) A screen-printed carbon electrode modified with a bismuth film and gold nanoparticles for simultaneous stripping voltammetric determination of Zn (II), Pb (II) and cu (II). Microchim Acta 184:4731–4740
26. Lee S, Park SK, Choi E, Piao Y (2016) Voltammetric determination of trace heavy metals using an electrochemically deposited graphene/bismuth nanocomposite film-modified glassy carbon electrode. J Electroanal Chem 766:120–127
27. Guo Z, Luo XK, Li YH, Zhao QN, Li MM, Zhao YT, Ma C (2017) Simultaneous determination of trace Cd (II), Pb (II) and Cu (II) by differential pulse anodic stripping voltammetry using a reduced graphene oxide-chitosan/poly-l-lysine nanocomposite modified glassy carbon electrode. J Colloid Interface Sci 490:11–22
28. Lin H, Li M, Mihailovič D (2015) Simultaneous determination of copper, lead, and cadmium ions at a Mo_6S_9-xIx nanowires modified glassy carbon electrode using differential pulse anodic stripping voltammetry. Electrochim Acta 154:184–189
29. Ruecha N, Rodthongkum N, Cate DM, Volckens J, Chailapakul O, Henry CS (2015) Sensitive electrochemical sensor using a graphene–polyaniline nanocomposite for simultaneous detection of Zn (II), Cd (II), and Pb (II). Anal Chim Acta 874:40–48
30. Sahoo PK, Panigrahy B, Sahoo S, Satpati AK, Li D, Bahadur D (2013) In situ synthesis and properties of reduced graphene oxide/Bi nanocomposites: as an electroactive material for analysis of heavy metals. Biosens Bioelectron 43:293–296
31. Lee S, Oh J, Kim D, Piao Y (2016) A sensitive electrochemical sensor using an iron oxide/graphene composite for the simultaneous detection of heavy metal ions. Talanta 160:528–536
32. Wang WJ, Cai YL, Li BC, Zeng J, Huang ZY, Chen XM (2018) A voltammetric sensor for simultaneous determination of lead, cadmium and zinc on an activated carbon fiber rod. Chin Chem Lett 29:111–114
33. Devadas B, Sivakumar M, Chen SM, Rajkumar M, Hu CC (2015) Simultaneous and selective detection of environment hazardous metals in water samples by using flower and Christmas tree like cerium hexacyanoferrate modified electrodes. Electroanalysis 27:2629–2636
34. Prabakar SR, Sakthivel C, Narayanan SS (2011) Hg (II) immobilized MWCNT graphite electrode for the anodic stripping voltammetric determination of lead and cadmium. Talanta 85:290–297
35. Lezi N, Economou A, Dimovasilis PA, Trikalitis PN, Prodromidis MI (2012) Disposable screen-printed sensors modified with bismuth precursor compounds for the rapid voltammetric screening of trace Pb (II) and Cd (II). Anal Chim Acta 728:1–8